

Highlights

Reducing RES Droughts through the integration of wind and solar PV

Boris Morin, Aina Maimó Far, Damian Flynn, Conor Sweeney

- RES droughts are analysed using 45 years of hourly wind and solar PV generation data
- RES droughts from C3S-Energy and ERA5-Atlite datasets are compared
- Adding solar PV to a wind-dominated system reduces RES drought frequency and duration
- Validated RES datasets are crucial to accurately identify RES drought extremes

Reducing RES Droughts through the integration of wind and solar PV

Boris Morin^{a,*}, Aina Maimó Far^a, Damian Flynn^b, Conor Sweeney^a

*^aSchool of Mathematics and Statistics, University College Dublin, Belfield, Dublin
4, Dublin, D04 V1W8, Ireland*

*^bSchool of Electrical and Electronic Engineering, University College Dublin, Belfield,
Dublin 4, Dublin, D04 V1W8, Ireland*

*Corresponding author

Email addresses: `boris.morin@ucdconnect.ie` (Boris Morin),
`aina.maimofar@ucd.ie` (Aina Maimó Far), `damian.flynn@ucd.ie` (Damian Flynn),
`conor.sweeney@ucd.ie` (Conor Sweeney)

Abstract

Increasing the share of electricity produced from renewable energy sources (RES), combined with RES dependence on weather, poses a critical challenge for energy systems. This study investigates the importance of the balance between wind and solar photovoltaic (PV) capacity on periods of low renewable generation, known as RES droughts. Three different RES datasets are used to estimate the capacity factors for different scenarios of installed capacities for wind and solar PV power. The skill of the RES models is quantified by comparing capacity factor time series to observed hourly data and by assessing their representation of observed RES droughts. The RES models are used to generate a 45-year hourly time series of RES capacity factor, enabling analysis of the frequency, duration and return periods of RES droughts at a climatological scale. Results show the importance of using an accurate, validated RES model for RES drought risk assessment. The addition of solar PV capacity to a wind-dominated system results in a significant reduction in the frequency and duration of RES droughts, while also reducing extremes and seasonal RES drought patterns. These findings underscore the importance of diversification in RES capacity to enhance energy security and resilience.

Keywords: RES Drought, Wind Power, Solar PV Power, Renewable Energy Sources, Return Periods

1. Introduction

The EU aims to generate at least 69% of its electricity from renewable energy sources (RES) by 2030, up from 41% in 2022 [1]. While this transition is essential for reducing greenhouse gas emissions, it also highlights the challenge of managing the variability of weather-dependent energy sources such as wind and solar photovoltaic (PV) power. This challenge is amplified by the increasing electrification of energy sectors, which places greater demand on the power system and makes it more sensitive to meteorological conditions, both in historical [2] and future climates [3]. Periods of low renewable generation, known as *Dunkelflaute* or RES droughts, pose significant risks to system adequacy and energy security, emphasising the need for a resilient energy system to meet both growing electricity demand and decarbonisation targets.

RES drought events do not have a fixed definition, with various approaches present in the literature. One common method defines a RES drought as a period during which the average capacity factor (CF) remains below a fixed threshold for a specified duration. For example, Kaspar et al. [4] used this method to investigate the shortfall risks of low wind and solar PV generation in Europe, with a focus on Germany, testing multiple CF thresholds and durations. Similarly, Mockert et al. [5] examined the link between weather regimes and RES droughts in Germany using a 48-hour rolling window under a threshold to define RES droughts. Similar fixed-threshold approaches have also been applied using CF series reconstructed through machine learning in regions such as Japan [6] and Hungary [7].

Alternative methods adjust the CF threshold dynamically over the year to account for seasonal variations in renewable production. Raynaud et al. [8] defined RES droughts as sequences of days with renewable electricity generation below a threshold that varies seasonally, a methodology later adapted for India [9]. Building on this, Kapica et al. [10] compared the likelihood of increased RES droughts in Europe under different climate models. Other studies have defined RES droughts based on deviations from daily mean production: Rinaldi et al. [11] applied these in the U.S. Western Interconnection to quantify the benefits of long-term storage, while Brown et al. [12] examined weekly timescales to explore meteorological influences on the most severe RES drought events. Another method defines RES drought indices based on metrics commonly used in hydro-meteorology to characterise RES droughts [13]. This approach identifies periods of unusually low generation relative to historical production levels, using the lowest production percentiles. Bracken et al. [14] used this approach to analyse RES droughts at different time scales in the U.S. [14], and Lei et al. [15] used it to quantify RES droughts in wind-PV-hydro systems in China.

In addition to examining periods of low renewable electricity generation, several studies also explore the periods when the imbalance between renewable generation and electricity demand (residual load) is high. Raynaud et al. [8] showed the difference between RES droughts and high residual load events in a hypothetical fully renewable system composed of wind, solar PV and run-of-the-river hydropower. Similarly, Allen and Otero [13] also defined a standardised index based on meteorological droughts to address residual load, whose correlation to the electricity generation index is mostly negative (as expected, although quite low anticorrelations and even small positive correlations appear for some European countries). This index was also applied

to the U.S. by Bracken et al. [14], revealing a consistent increase in the RES drought magnitude when load is considered, despite showing differing results across regions.

In this paper, the focus is exclusively on renewable electricity generation, which allows us to maintain physical models that do not consider the behavioural influence of demand. A fixed threshold approach is used to define RES droughts, which facilitates consistent inter-comparison between scenarios with different installed wind and solar PV capacities. The case study used in this paper is Ireland, a region with a strong reliance on wind power and ambitious targets for solar PV power expansion. This provides valuable insights into the potential benefits of diversifying the share of wind and solar PV on RES droughts.

RES droughts are identified using onshore wind and solar PV CF time series. In this study, three different datasets are used and compared, all of which are driven by the ERA5 reanalysis [16]. Two of the datasets are part of C3S Energy (C3SE), an energy-based operational dataset produced by the EU Copernicus Climate Change Service [17]. One of the C3SE datasets provides CF time series aggregated at the national scale, while the other provides the CF time series at each grid point, at the ERA5 resolution of 0.25° . The third dataset produced by the authors was generated using the Atlite model [18], which converts the ERA5 atmospheric data to a generation time series using specified wind turbine and PV panel models. Atlite is an open-source tool developed by PyPSA [18] and has been used for estimating wind and solar PV generation in order to study RES droughts in Germany [5].

Generic datasets for wind and solar PV CF are often used for the quantification of RES droughts. Despite undergoing a validation process, they are often not fully representative of each geographical location, and can show differences in the number of RES drought events [19]. This study evaluates the skill of a dataset developed for the European region (C3SE) when applied to a specific country (Ireland). In particular, the analysis explores the impact of using a generic versus a tailored dataset on RES drought assessments, in the context of a transition from a wind-dominated system to one with a greater share of solar PV.

The aim of this study is to answer three questions which are relevant for systems with a large share of RES generation:

- Do generic datasets have sufficient skill to reliably quantify extreme RES drought events?

- 89 • What is the importance of using accurate RES farm locations, and
90 regionally-validated wind and solar PV models, when analysing of RES
91 droughts?
- 92 • How does the integration of solar PV into a predominantly wind-based
93 system alter the characteristics of RES drought events?

94 The datasets used in this study are detailed in section 2, which describes
95 their characteristics and relevance for evaluating RES droughts. Section 3
96 outlines the RES datasets used to simulate wind and solar PV generation and
97 provides the methodology for defining and identifying RES drought events,
98 including the thresholds and metrics applied. In section 4, the datasets are
99 first verified against observed energy data to assess their accuracy, followed by
100 an analysis of RES drought occurrences for two scenarios with different ratios
101 of installed wind to solar PV capacities. Finally, section 5 offers a discussion
102 of the results in the context of energy reliability and future planning, followed
103 by the main conclusions and recommendations for further research.

104 **2. Data**

105 This study uses publicly available datasets to construct and validate the
106 datasets for estimating the CF of wind and solar PV power. The primary
107 data sources include: EirGrid and SONI, the transmission system operators
108 (TSO) for the Republic of Ireland and Northern Ireland, respectively; the
109 ERA5 reanalysis dataset; and the C3SE dataset.

110 *2.1. Wind and solar PV Capacity and Availability*

111 EirGrid, the TSO for the Republic of Ireland, and SONI, the Northern
112 Ireland TSO, provide detailed datasets on all wind and solar PV farms across
113 the island of Ireland (Republic of Ireland and Northern Ireland) from 1990
114 to the present [20]. These datasets include information such as each farm’s
115 installed capacity, name, and connection date. To enhance the accuracy of
116 this data, the longitude and latitude for each farm were manually determined
117 through online searches. For simplicity, this data will be referred to as orig-
118 inating from EirGrid, as all-island data was directly obtained from EirGrid,
119 and the combined regions of the Republic of Ireland and Northern Ireland
120 will be referred to as Ireland throughout the remainder of this document.

121 The spreadsheet available from the EirGrid website contains two key vari-
122 ables: generation and availability. Generation is the energy that a RES farm

123 actually contributed to the grid, which may include limitations introduced
124 by the TSO to maintain grid stability, such as constraints and curtailment.
125 Availability represents the energy that would have been generated from a RES
126 farm if no grid constraints had been applied, making it representative of the
127 weather-related response. Generation and availability values are available
128 from 2014 onward for wind power and from 2018 onward for solar PV power,
129 although solar PV availability data only became present in the Republic of
130 Ireland in 2023. This study focuses on availability for all analyses.

131 2.2. Atmospheric Variables

132 All of the datasets used in this study are driven by data from the ERA5 re-
133 analysis [16], produced by the European Centre for Medium-Range Weather
134 Forecasts (ECMWF). This global gridded dataset provides hourly atmo-
135 spheric variables from 1940 to the present at a horizontal resolution of 0.25° .
136 Table 1 lists the relevant ERA5 variables.

Table 1: ERA5 variables used to calculate wind and solar PV generation

ERA5 name	variable
100 metre zonal and meridional wind speed	u_{100}, v_{100}
2 metre temperature	$t2m$
Surface net solar radiation	ssr
Surface solar radiation downwards	$ssrd$
Top of atmosphere incident radiation	$tisr$
Total sky direct solar radiation at surface	$fdir$

137 2.3. C3S Energy

138 The EU Copernicus Climate Change Service developed the C3S-Energy
139 (C3SE) renewable energy dataset for Europe [17], using ERA5 atmospheric
140 variables and weather-to-energy models. This dataset provides hourly CF for
141 wind and solar PV power from 1979 to the present. The data are available
142 on the same grid as the ERA5 data, which has a horizontal resolution of
143 0.25° . The time series are also available for download at two aggregated
144 scales: regional (NUTS 2) and national.

145 The wind CF in C3SE was calculated using wind speeds at 100 metres
146 (u_{100}, v_{100}) and a standard turbine model, the Vestas V136/3450, with a fixed
147 hub height of 100 meters. As data on wind turbine fleet locations and speci-
148 fications are difficult to obtain across Europe, C3SE assumes a homogeneous

149 distribution of wind turbines across the ERA5 grid. While this approach
150 does not capture the precise capacity factors reported by grid operators, it
151 provides a well-correlated time series that effectively represents the impact
152 of climate variability on wind power generation. The C3SE solar PV CF was
153 also calculated for the ERA5 grid. It is derived from meteorological data, in-
154 cluding surface solar radiation downwards (*ssrd*) and air temperature (*t2m*),
155 using a reference solar PV plant model. This model incorporates empirical
156 calculations for key system components such as optical losses, module effi-
157 ciency, and inverters. The final CF accounts for a mix of module orientations
158 typical for each location [21].

159 3. Methods

160 This study analyses RES droughts across the island of Ireland using on-
161 shore wind and solar PV CF time series from three datasets: two from C3SE,
162 based on national-level data (C3S NAT) and grid-level data (C3S GRD), and
163 one derived from the Atlite model (ATL). Fig. 1 presents the statistics of the
164 three datasets in violin plots for wind and solar PV. These plots illustrate the
165 density of CF values over time, highlighting differences between the datasets
166 and their alignment with observed data.

167 3.1. C3S Energy National: C3S NAT

168 The C3S NAT dataset is created by combining two inputs provided by
169 C3SE at the corresponding NUTS levels: Republic of Ireland (NUTS0: IE)
170 and Northern Ireland (NUTS2: UKN0). The two inputs are combined, using
171 the actual installed capacity as weights. This dataset assumes that RES
172 generation occurs at every ERA5 grid point in Ireland.

173 3.2. C3S Energy Gridded: C3S GRD

174 The C3S GRD dataset uses, as inputs, the actual locations of the RES
175 farms in Ireland, and the CF from C3SE over the ERA5 grid. For each
176 farm, the CF from the nearest grid point on the C3SE dataset was selected.
177 A weighted average of the CF associated with each farm, using the farm's
178 installed capacities, was used to produce the total CF time series.

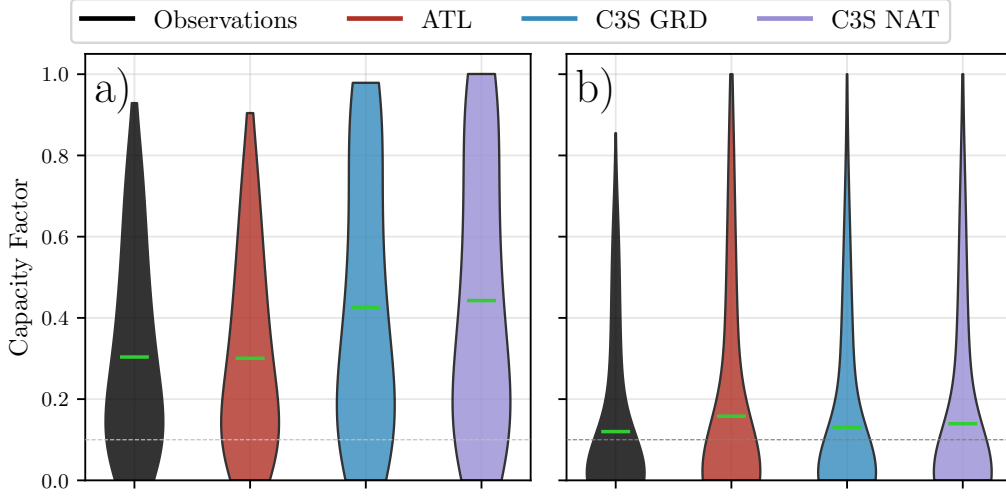


Figure 1: Violin plots of CF distributions for wind a) and solar PV b) datasets. Each violin represents the distribution of CF over time for different datasets: Observations (black), ATL (red), C3S GRD (blue), and C3S NAT (purple). The mean value for each dataset is marked with a green horizontal line. The red line indicates the threshold of 0.1 used in the study to identify RES droughts

179 3.3. Atlite: ATL

180 The ATL dataset is produced using the Atlite model. Atlite allows the
 181 user to define the wind turbine power curve and PV panel model to use
 182 when converting weather variables to wind and solar PV generation. The
 183 Atlite model takes as inputs the locations of RES farms and ERA5 weather
 184 variables: wind speed at 100 metres (u_{100} , v_{100}) for wind generation, and
 185 radiation variables (ssr , $ssrd$, $tisr$, and $fdir$) along with air temperature
 186 ($t2m$) for solar PV generation. The output of the Atlite model is a generation
 187 time series, which is divided by the total capacity to transform it back into
 188 CF. The selection of the wind turbine power curve and PV panel model
 189 represents the key difference between this dataset and C3S GRD. This study
 190 identifies the most appropriate wind turbine power curve to use from the
 191 121 power curves, each at five different levels of smoothing, made available
 192 by Renewables.ninja [22], and selects the PV panel model out of the options
 193 available within Atlite.

194 3.4. Energy Scenarios

195 The three datasets provide CF time series for both wind and solar PV. In
 196 addition to analysing the CF of wind and solar PV separately, a combined
 197 CF was computed for each dataset by averaging wind and solar PV CF,
 198 weighted by their installed capacities at the end of 2023 (5.9 GW for wind
 199 power and 0.6 GW for solar PV power). This configuration is referred to as
 200 the 91W-9PV scenario, reflecting the distribution of 91% wind and 9% solar
 201 PV capacity. Given that solar PV capacity in Ireland is low in 2023, and to
 202 explore how a more balanced distribution of wind and solar PV capacities
 203 might impact RES droughts, this study also considered a second scenario,
 204 referred to as 57W-43PV, where the installed solar PV capacity is assumed
 205 to increase to 8.6 GW, while wind capacity rises to 11.45 GW. These values
 206 are based on targets outlined in the roadmap published by the 2024 Climate
 207 Action Plan [23]. This study does not include offshore wind in the analysis.
 208 Recent reports suggest that even by 2030, Ireland is unlikely to have any
 209 significant new offshore wind farms, with projected offshore capacity expected
 210 to remain near zero using realistic scenarios [24].

211 New time series were generated for both the ATL and C3S GRD solar
 212 PV datasets, incorporating a revised distribution of installed capacity across
 213 Ireland as specified in the roadmap. For wind power, the CF time series
 214 remains unchanged, as significant shifts in the location of wind farms are not
 215 expected. In total, twelve CF time series were analysed in this study, six for
 216 individual wind and solar PV CF (three datasets for each source) in the 91W-
 217 9PV scenario, and an additional six time series that include the combined
 218 CF for 91W-9PV and 57W-43PV scenarios across the different datasets.

219 It is important to note that the specific capacity values used in this study
 220 are illustrative and are not intended to reflect precise future realities. Instead,
 221 they serve to explore the impact of transitioning from a wind-dominated sys-
 222 tem (91W-9PV) to a more evenly distributed system (57W-43PV). This ap-
 223 proach allows for a comparative analysis between the two scenarios, assessing
 224 how the balance of RES capacity affects the occurrence of RES droughts.

225 For each dataset (ATL, C3S GRD, and C3S NAT), four distinct scenarios
 226 are examined, as summarised below:

- 227 • Wind Power - based on the actual capacity at the end of 2023
- 228 • Solar PV Power - based on the actual capacity at the end of 2023

- Combined RES / 91W-9PV - based on the actual capacity at the end of 2023
- Combined RES / 57W-43PV - based on the projected capacity for 2030

3.5. RES Drought Definition

In this study, a RES drought event was defined as occurring when the 24-hour moving average of CF remains below a fixed threshold of 0.1 for a period of longer than 24 hours. By using a 24-hour moving average, fewer but longer-lasting events were captured compared to using the raw CF time series, which can be more sensitive to short-term fluctuations. The 24-hour rolling average also avoids potential masking of day-long events due to their start time. A fixed threshold approach was chosen in this study to enable consistent inter-comparison between datasets.

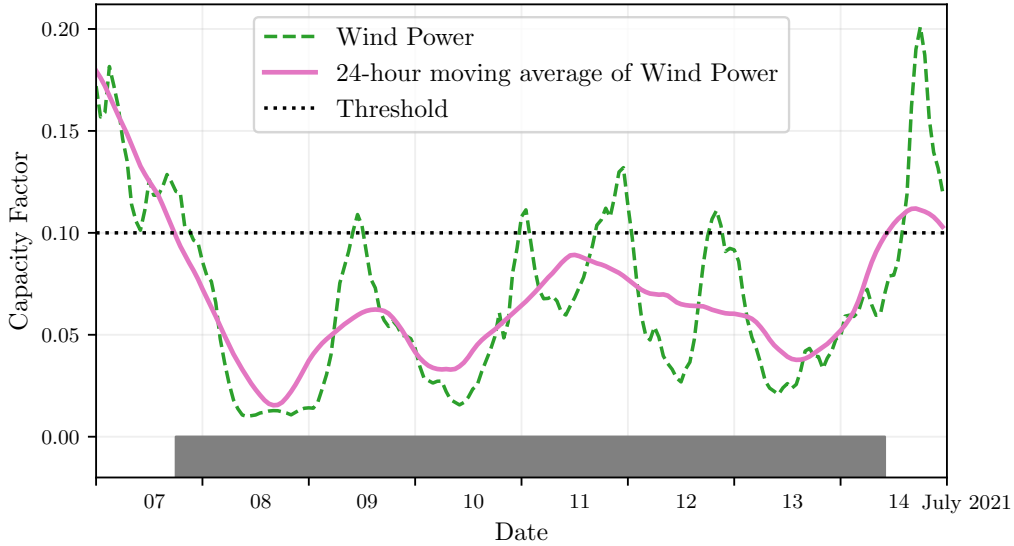


Figure 2: Wind time series of CF (green) and its 24-hour moving average (pink) from the 7th to the 15th of July 2021. The black dashed line indicates the CF threshold. The grey bar shows the period identified as a wind drought under our definition

The moving average approach smooths out short-term fluctuations, so that brief periods above the threshold do not interrupt an otherwise continuous low-CF period (Fig. 2). This means that a single hour above the threshold does not "break" a drought event if it is surrounded by prolonged

low-generation hours. As a result, fewer but longer-lasting drought events are identified, which may better reflect real-world conditions where energy supply constraints persist over extended periods.

4. Results

4.1. Verification

The accuracy of the datasets used in this study was verified, before continuing to the analysis of RES droughts. For the verification process, time-varying values of installed capacity were used to account for changes in RES development over the verification period. This step allowed us to assess how well the datasets represent the production of renewable energy by comparing them against observed data.

4.1.1. Wind Energy

The C3S datasets use the Vestas V136/3450 wind turbine power curve (Fig. 3a). The Atlite model allows the user to specify the power curve. We considered the 121 power curves available for download from Renewables.ninja [22]. For each power curve, Renewables.ninja also provides four associated smoothed power curves. The smoothing is done using a Gaussian filter with different standard deviations that depend on the wind speed. A separate wind CF time series for Ireland was generated for each of the wind turbine power curves and smoothing levels.

The performance of each CF time series is then assessed based on four skill scores: correlation coefficient (CC), root mean square error (RMSE), mean bias error (MBE), and the percentage of overlap. The percentage of overlap quantifies the similarity between the observed and modelled distributions. It is a positively oriented skill score, where 100% shows full agreement between the two distributions, and 0% indicates no overlap. The histograms of hourly CF values for the most recent decade (2014-2023) are used to calculate this skill score.

Based on these metrics, the most representative power curve for Ireland is the Enercon E112.4500 power curve with the $0.3w$ smoothing filter. The smoothing of the wind turbine power curve represents losses associated with each turbine, as well as losses such as wake effects between turbines, which are important when modelling wind energy on larger spatial scales. The histogram in Fig. 3b shows that the C3SE power curve tends to underestimate low CF values and overestimate higher ones, whereas the smoothed ATL

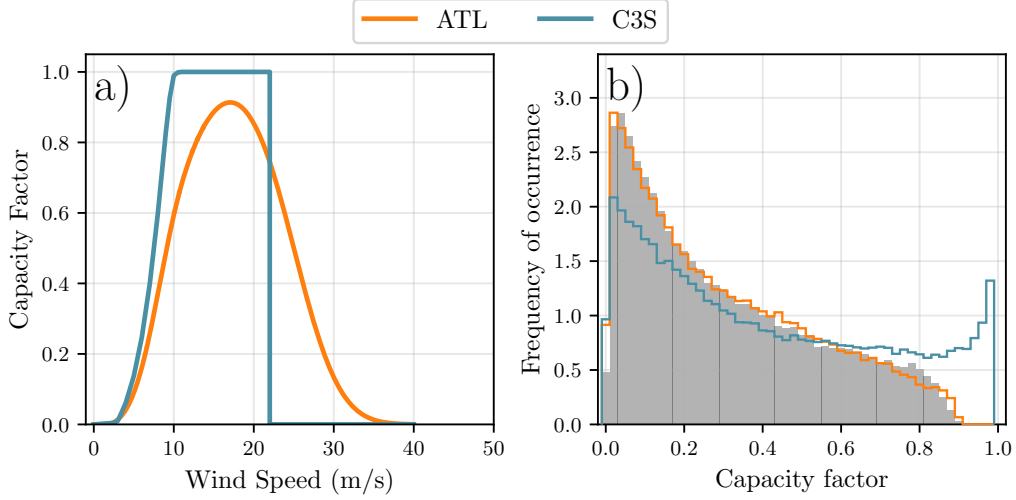


Figure 3: a) Power curves of the Enercon E112.4500 with a 0.3w smoothing filter used by ATL (orange) and the Vestas V136/3450 used by C3SE (blue) b) Histograms of wind CF for Ireland from ATL (orange), C3SE (blue) and Observed (shaded)

280 power curve more closely follows the observed wind availability data. This
 281 is further supported by the percentage of overlap which is higher for ATL
 282 (97.2%) than for C3SE (83.2%), indicating better agreement with observed
 283 data.

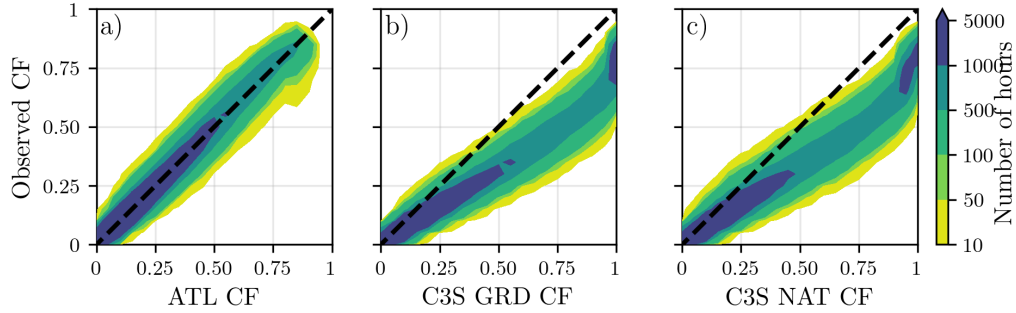


Figure 4: Wind CF density plot of the observed CF (vertical axes) and modelled (horizontal axes) CF data for the a) ATL, b) C3S GRD and c) C3S NAT datasets

284 The effect of the difference between the power curves is also visible in
 285 Fig. 4, which shows a density plot of wind CF values. The two C3S datasets

are shown to overestimate the observed CF, whereas the ATL dataset is in good agreement with the observed data. The skill scores presented in Table 2 show that ATL performs better than the two C3S datasets for all of the skill scores.

	ATL	C3S GRD	C3S NAT
CC	0.981	0.972	0.970
RMSE	0.045	0.177	0.162
MBE	-0.003	0.137	0.121

Table 2: Skill scores for wind power for the three datasets compared to observed data

Fig. 5 shows the average annual number of wind drought events during the 2014 to 2023 validation period. The figure reveals that ATL presents the best overall agreement with the observed frequency and duration of wind drought events. This pattern is particularly evident for shorter-duration events, which are the most frequent.

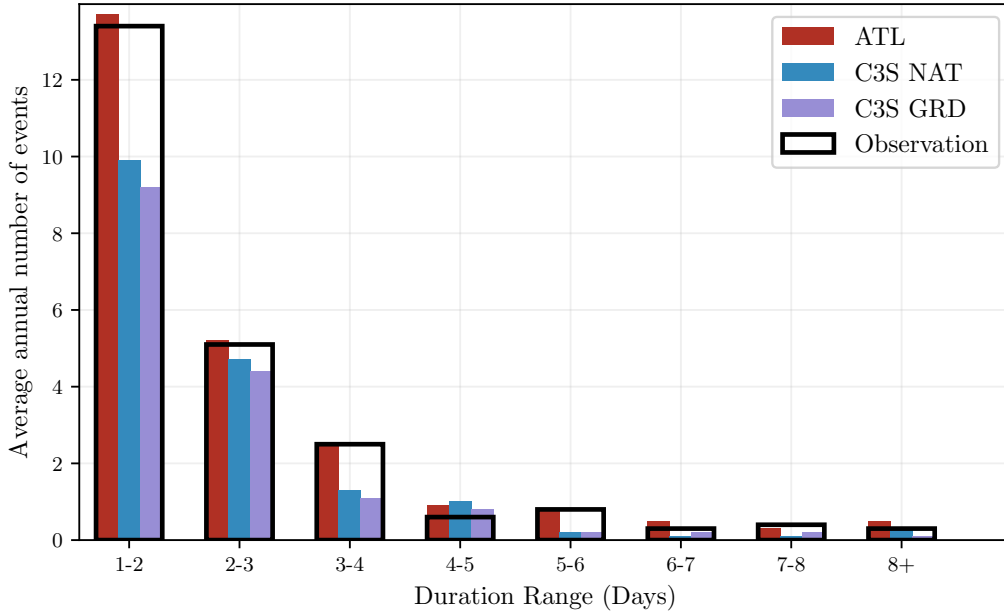


Figure 5: Average annual number of wind drought events for ATL (red), C3S GRD (blue), C3S NAT (purple), and the observed data (black outline). The wind droughts are identified from 2014 to 2023, considering the actual capacity of the system at any given time

295 This verification for wind generation data highlights the importance of
 296 selecting a representative wind turbine power curve for the region being anal-
 297 ysed. The ATL dataset, which uses a representative wind turbine power
 298 curve, is skilled at reproducing wind CF and RES droughts over Ireland. On
 299 the other hand, the power curve used for both C3S GRD and C3S NAT is
 300 not representative for Ireland, as it severely overestimates generation, under-
 301 estimating the occurrence of RES droughts. This highlights a problem with
 302 using generalised datasets for analysing RES droughts: biases severely affect
 303 their ability to accurately reproduce RES drought events. The skill scores
 304 for the three datasets (Tab. 2) show only a small difference in their ability to
 305 reproduce the changes in CF, as seen by their similar CC scores. However,
 306 their ability to reproduce the actual CF values is much lower than that of
 307 ATL, with RMSE scores almost four times bigger for the two C3S datasets.
 308 There is a clear bias towards an overestimation of CF, seen in the MBE val-
 309 ues, which leads to the underestimation of RES droughts. This highlights
 310 the need to use regionally verified models to assess RES droughts.

311 4.1.2. Solar PV Energy

312 The Atlite model allows the user to select certain PV panel characteristics.
 313 In this study, the three PV panel types available in the Atlite model were
 314 considered (CSi, CdTe, Kaneka). Following the same methodology as in the
 315 previous section, the three available models were compared using four skill
 316 scores (CC, RMSE, MBE, and the percentage of overlap). Based on the best-
 317 performing metrics, the Beyer PV panel model was selected [25], using the
 318 Kaneka Hybrid panel option. For all solar PV farm locations, the azimuth
 319 angle is fixed at 180° (due south), and the optimal tilt angle option is applied.

320 The solar PV installed capacity available on the spreadsheets from Eir-
 321 Grid represents the Maximum Export Capacity (MEC) and does not ac-
 322 curately reflect the installed solar PV capacity. To enable actual solar PV
 323 generation potential to be modelled correctly, installed capacities were set at
 324 1.4 times the MEC values. This scaling factor was estimated by analysing
 325 proprietary data from individual solar PV farms provided by EirGrid, which
 326 showed that, on average, assuming that the installed capacities of farms ex-
 327 ceed their MEC values by 40% yields the best agreement with the observed
 328 availability.

329 Fig. 6 shows that the three datasets have a similar tendency to overesti-
 330 mate the CF compared to the observed values, especially for high CF values.
 331 The skill scores presented in Table 3 indicate that C3S GRD and C3S NAT

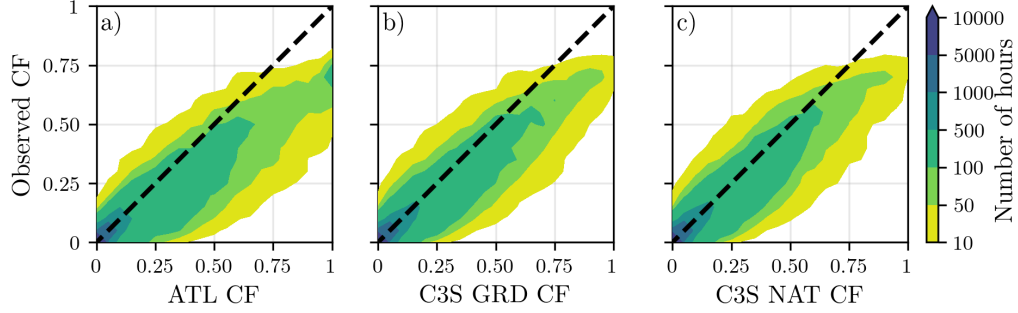


Figure 6: Solar PV CF density plot of the observed (vertical axes) and modelled (horizontal axes) CF series for the a) ATL, b) C3S GRD and c) C3S NAT datasets

perform better than ATL for solar PV CF, with lower RMSE and MBE, and higher CC scores. This may be due to the statistical approach taken by C3SE for the orientation of the PV panels.

	ATL	C3S GRD	C3S NAT
CC	0.921	0.931	0.931
RMSE	0.119	0.090	0.113
MBE	0.046	0.027	0.021

Table 3: Skill scores for solar PV CF for the three datasets compared to observed data

Fig. 7 shows the number of solar PV drought events during the 2023 validation period across different duration ranges. The figure reveals partial agreement between the three datasets and the observed data, with consistent results noticed for duration ranges of 1-2, 3-4, 7-8, and 8+ days. However, discrepancies appear in the other ranges, where the models diverge from the observed data. The main challenge in validating solar PV data stems from the recent installation of a large share of Ireland’s solar PV capacity, with over 65% of the total solar PV capacity installed in 2023. This results in uncertainties in solar PV generation data and the actual generating capacity in the first few months after each farm is connected. Overall, C3S GRD performs slightly better than the other datasets in reproducing observed solar PV drought events.



Figure 7: Number of solar PV drought events for ATL (red), C3S GRD (blue), and C3S NAT (purple) and the observed data (black outline). The solar PV droughts are identified for 2023, considering the actual capacity of the system at any given time

4.2. Analysis

In this section, RES droughts are analysed by calculating the frequency and duration of RES drought events, the return periods for different RES drought durations, and the seasonality of RES drought events. Understanding the characteristics and timing of RES drought events enables system operators to optimally plan for reserve capacity requirements, ensuring grid stability and security of supply. Results are presented for the three datasets, allowing their differences on the characterisation of RES droughts to be clearly identified.

RES drought events are evaluated under two different scenarios with fixed installed capacities: the 91W-9PV scenario, with 5.9 GW of wind capacity and 0.6 GW of solar PV capacity; and the 57W-43PV scenario, where wind capacity comprises 11.45 GW and solar PV capacity increases to 8.6 GW. Both scenarios were driven by 45 years of ERA5 data. Using the RES drought identification process described in Section 3.5, wind and solar PV droughts are first analysed separately before presenting the results for combined (wind

363 + solar PV) RES droughts under both scenarios.

364 4.2.1. Annual Number of RES Droughts

365 The first part of the analysis examines the annual number of RES drought
366 events. When only wind energy is considered (Fig. 8a), the number of RES
367 drought events decreases as the duration range increases, with very few events
368 lasting more than seven days. In contrast, for solar PV energy (Fig. 8b), RES
369 drought frequency declines from one to eight days and then slightly increases
370 for longer durations. This behaviour is attributable to Ireland’s high-latitude
371 location, where reduced sunlight in winter (from November to March) leads
372 to consistently low solar PV output.

373 Moreover, the comparison between wind and solar PV results indicates
374 that the median, first, and third quartiles for solar PV are consistently higher
375 than or equal to those for wind. This is expected, given that solar PV gener-
376 ation is inherently lower, zero at night, and limited by the solar cycle. When
377 wind and solar PV are combined under the 91W-9PV scenario (Fig. 8c), the
378 results closely mirror those of wind alone, due to the dominance of wind power
379 in the current energy mix. However, in the 57W-43PV scenario (Fig. 8d),
380 a marked reduction in RES drought events is observed across all datasets,
381 with a decrease of the total number of events of 56% for ATL, 52% for C3S
382 GRD, and 50% for C3S NAT, demonstrating the beneficial effects of a more
383 balanced energy mix.

384 The consistently higher RES drought counts reported by the ATL dataset,
385 compared to the C3S datasets, underscore the importance of wind turbine
386 power curve representation when quantifying RES droughts. Whereas the
387 three datasets agree on the overall effect of balancing the share of wind and
388 solar PV generation, they differ at a quantitative level, which has crucial
389 implications for energy planning.

390 4.2.2. Return Periods of RES Drought Duration

391 RES drought events identified over the 45-year period were used to cal-
392 culate the return periods for different RES drought durations. A return
393 period is the estimated average time interval between events of a specified
394 duration (not to be confused with the frequency of their occurrence within a
395 fixed time frame). Fig. 9 shows the return periods for different RES drought
396 durations, which can be used to capture the most extreme events affecting
397 the system. Understanding their return periods is crucial, as extreme yet
398 rare RES droughts pose the toughest challenge to energy security by placing

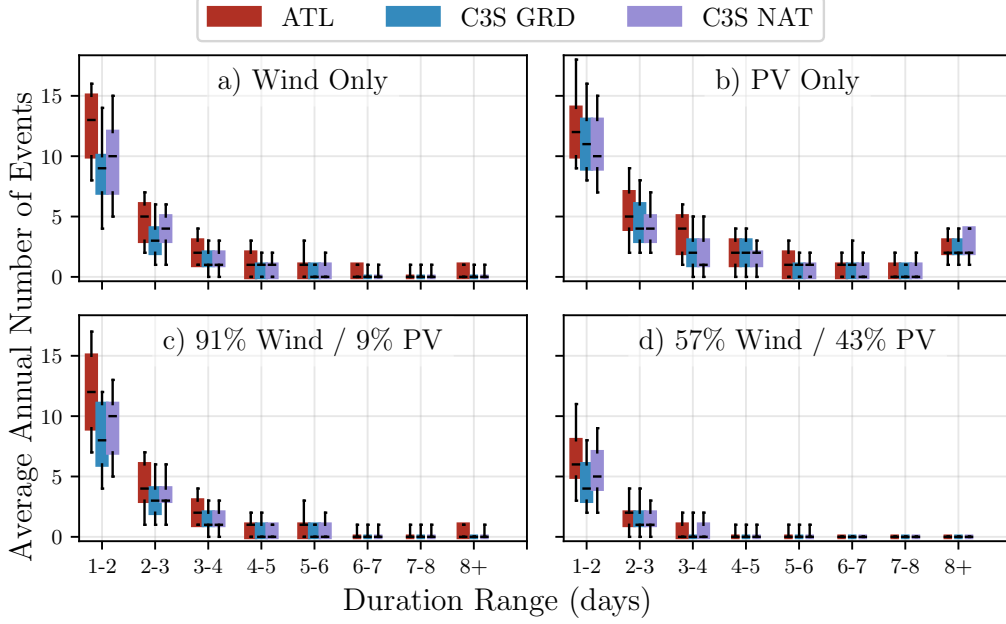


Figure 8: Average annual number of RES droughts (from 1979 to 2023) for a) Wind, b) solar PV, c) 91W-9PV and d) 57W-43PV for ATL (red), C3S GRD (blue), and C3S NAT (purple). The x-axis represents duration ranges in days (lower bound included), while the y-axis indicates the annual number of events. The boxes display the first and third quartiles and the median is marked by a black line. The whiskers indicate the 5th and 95th percentiles

399 significant strain on the conventional backup sources necessary to maintain
400 security of supply during these events.

401 The duration of wind droughts (Fig. 9a) increases in a log-linear fash-
402 ion across the three datasets. The log-linear trend indicates a predictable
403 relationship between drought duration and occurrence, with longer wind
404 droughts becoming exponentially less likely as duration increases. In the
405 case of solar PV droughts (Fig. 9b), Atlite behaves differently than the two
406 C3S datasets. The ATL dataset show a generally log-linear increase. For C3S
407 GRD and C3S NAT, the duration of PV droughts increases in a log-linear
408 pattern for events lasting less than 16 days. Beyond this duration, there is
409 a sharp rise in drought duration for events up to a one-year return period.
410 This sudden increase again reflects the impact of extended periods of low PV
411 generation during winter in Ireland. The difference between the ATL and

the C3S results arises from differences in the datasets near the threshold of 0.1 CF. ATL remains slightly above the threshold more frequently during these conditions, leading to shorter, more fragmented RES drought events. In contrast, C3S GRD and C3S NAT tend to fall below the threshold in similar conditions, resulting in longer continuous drought periods, especially during winter.

Under the 91W-9PV scenario (Fig. 9c), the combined RES drought return periods mirror those for wind alone, reflecting the dominance of wind in the current energy mix. In contrast, the 57W-43PV scenario (Fig. 9d) shows a dramatic increase in return periods across all durations, suggesting that a more diversified energy mix can substantially mitigate the frequency of prolonged drought events. For example, the return period for a five-day RES drought event (shown by the vertical dashed lines in Fig. 9) extends from roughly six months for the 91W-9PV scenario, to four years for the 57W-43PV scenario in the ATL dataset, and from about fifteen months to around five years in the two C3S datasets. Despite the lower wind share in the 57W-43PV scenario, typically known for its relative stability, the balanced share with solar PV leads to extended return periods for RES droughts. This result indicates that the complementarity between wind and solar PV plays a crucial role in reducing the occurrence of RES drought events in a diversified energy portfolio.

Across Fig. 9a, c, and, d, the return periods in the ATL dataset are consistently higher than those in the two C3S datasets. For instance, in the 91W-9PV scenario (Fig. 9c), an event with a one-year return period lasts six days in the ATL dataset, compared to only five days in the C3S datasets. This difference underscores the importance of model selection when quantifying RES droughts, as each dataset's assumptions and parametrisations significantly influence RES droughts duration estimates. Additionally, in all four graphs, the similarity between results from the two C3S datasets suggests that assumptions in the ATL dataset, such as wind turbine power curve selection and PV panel specifications, have a greater impact on RES drought duration estimates than the precise geographic distribution of RES farms when studying the return periods of RES droughts.

The return periods calculated from the three datasets show large differences, in particular for the more extreme events with longer return periods. The C3S datasets produce shorter RES drought durations for these events, which would have the largest impact on the power system. This shows that system planning based on the wrong datasets could yield an underestimation

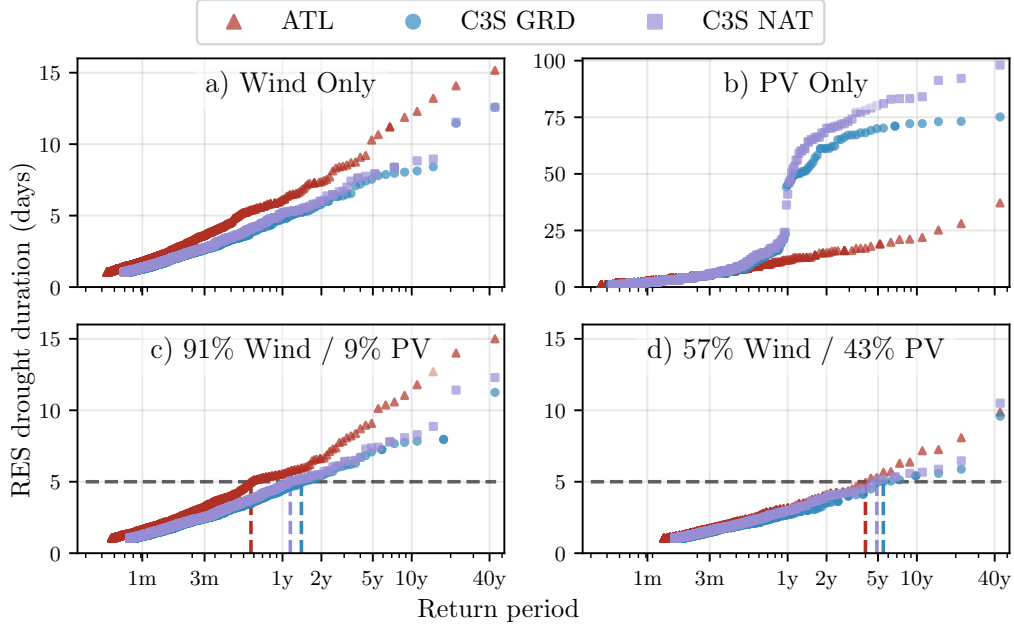


Figure 9: Return periods of the duration of RES droughts (from 1979 to 2023) for a) Wind, b) Solar PV, c) 91W-9PV and d) 57W-43PV for ATL (red triangle), C3S GRD (blue circle), and C3S NAT (purple square). The x-axis represents the return period time in a log-scale and the y-axis indicates the duration of RES drought associated with it. The horizontal dashed line marks the 5-day return period, with coloured vertical dashed marking its return period for each dataset

450 of the duration of extreme RES droughts, potentially leading to shortages
 451 linked to undersized reserve capacity.

452 4.2.3. Seasonal Distribution of RES Droughts

453 The seasonal analysis of RES droughts is based on the percentage of hours
 454 in each month classified as part of a RES drought event. Wind droughts tend
 455 to be more frequent during summer, whereas solar PV droughts are more
 456 common in winter due to reduced sunlight. By comparing these seasonal
 457 patterns across different datasets and energy scenarios, this study examines
 458 how model-specific assumptions and variations in capacity mix affect the
 459 overall characterisation of RES drought events.

460 For the wind-only scenario (Fig. 10a), the ATL dataset exhibits a pro-
 461 nounced seasonal pattern, with about 24% of summer hours (June, July,
 462 August) identified as RES droughts compared to only 4% in winter (Decem-

ber, January, February). This strong seasonal signal is less evident in the C3S datasets, which suggests that the differences in the underlying wind power curves play a significant role. In ATL, CF near or below the 0.1 threshold occurs at relatively higher wind speeds, resulting in a higher count of RES drought hours during the summer months. In contrast, solar PV droughts (Fig. 10b) display an opposite seasonal trend. Across all datasets, over 60% of winter hours are classified as solar PV droughts, reflecting the naturally low solar irradiance in Ireland during winter.

ATL tends to record a slightly higher percentage of RES drought hours for wind and a marginally lower percentage for solar PV relative to the C3S datasets. These differences highlight how dataset-specific assumptions, such as the treatment of wind turbine power curves and PV panel characteristics, significantly influences the apparent seasonal dynamics of RES droughts.

The 91W-9PV scenario (Fig. 10c) shows patterns comparable to the ones for wind droughts (Fig. 10a). However, in the 91W/9PV scenario, the number of hours classified as RES droughts in summer decreases slightly compared to the wind-only scenario. This reduction can be explained by the contribution of solar PV generation during the summer months in the 91W-9PV scenario, even though it constitutes only 11% of total capacity. Since the number of RES drought hours for solar PV in summer is near zero, this small contribution has a noticeable impact on reducing overall RES drought hours. In the 57W-43PV scenario (Fig. 10d), all three datasets show a reduction in monthly RES drought frequency. Annual reductions in median RES drought frequency are observed across the datasets, dropping from 14% to 5% for ATL, from 8% to 3% for C3S GRD, and from 9% to 4% for C3S NAT. The balanced mix of wind and solar PV power in this scenario reduces the seasonal signal overall and significantly decreases the percentage of RES drought hours in the summer.

The seasonal variations of RES droughts observed in this study have important implications for energy planning. Energy demand peaks in winter for Northern European countries, making the seasonality of RES droughts critical for the sizing of reserve capacity. Our results show that selecting the wrong dataset could severely underestimate RES droughts during winter months, thereby affecting the reliability of the energy system during critical periods. Additionally, the integration of large shares of solar PV in the system leads to a generalised reduction of RES droughts, yet winter months present a slight increase. The natural limitations of solar PV lead to inevitably higher reserve capacity needs during winter months as reliance on RES in-

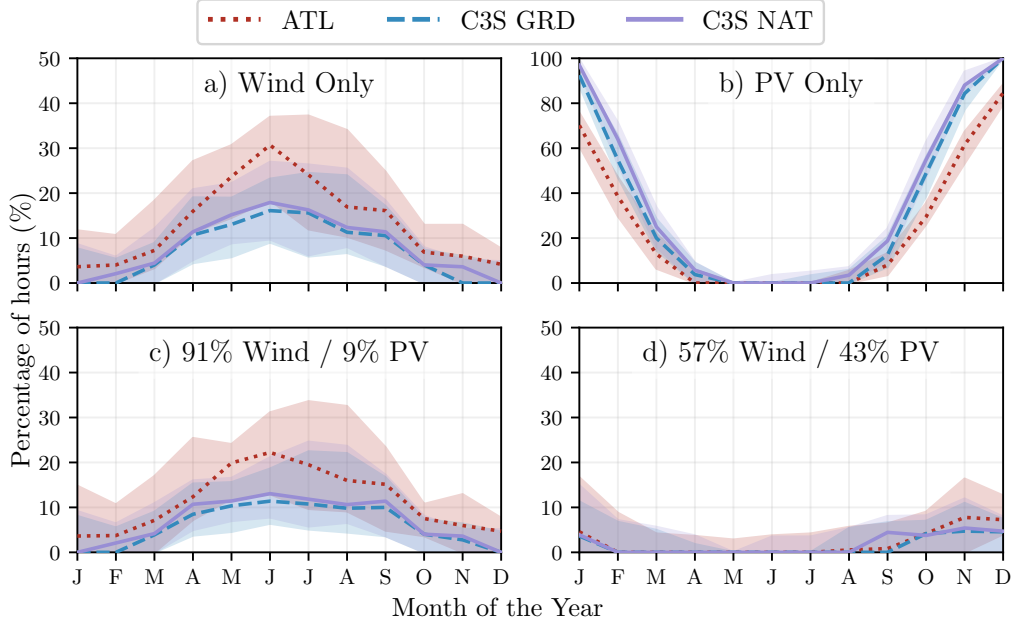


Figure 10: Percentage of hours in a month which are part of a RES drought (from 1979 to 2023) for a) Wind, b) Solar PV, c) 91W-9PV and d) 57W-43PV for ATL (red dotted), C3S GRD (blue dashed), and C3S NAT (purple solid). The x-axis represents the month of the year, and the y-axis indicates the percentage of hours. Lines correspond to the median values and the area between the first and third quartiles is shaded. Note the different y-axis scale for b).

creases. These types of insights are essential to develop targeted strategies that enhance grid resilience and ensure a stable energy supply throughout the year.

5. Conclusions

This study has explored the characterisation of RES droughts in the transition from a wind-dominated system to a more balanced system with integrated solar PV, based on the real case of Ireland. Three different datasets were compared over a 45-year period: one created using a regionally validated model and two derived from a generic dataset for Europe, C3S-Energy. The two datasets derived from C3S-Energy present different approaches, with one using large-scale aggregated information only, and the other one including the locations of farms as well. The regionally validated model considered the

513 locations of farms as well as tailored wind and solar PV models selected to
514 best represent the actual generation in Ireland.

515 Our results show the limitations in the quantification of RES droughts
516 present in datasets that have not undergone regional validation. The three
517 datasets used in this study are able to capture overall trends in RES drought
518 occurrence such as the seasonal cycle or the effect of increasing the share
519 of solar PV. However, significant differences in the quantitative values, par-
520 ticularly the extremes, emerge when using non-validated datasets for the
521 study of RES droughts. This finding highlights that using a non-validated
522 dataset can lead to undersized reserve capacity, with the associated negative
523 consequences for grid stability and security of supply.

524 This study has also revealed that differences in the wind turbine power
525 curves and solar PV panel models have a stronger influence on the esti-
526 mation of RES droughts than the consideration of RES farm locations. The
527 two datasets derived from C3S-Energy consistently underestimated the num-
528 ber of wind drought events and the frequency of extremes when compared
529 to the regionally validated dataset with a specifically selected wind turbine
530 power curve. This suggests that a meticulous selection of the wind turbine
531 power curve to match observed data is crucial for accurately quantifying RES
532 drought risks, thereby supporting more effective energy system planning.

533 Finally, the effect of the integration of solar PV in a wind-dominated
534 system on RES droughts has been explored in a real-case setting based on
535 Ireland. Our analysis has demonstrated that transitioning to a system with
536 similar amounts of wind and solar PV reduces the frequency, duration, and
537 seasonal variability of RES drought events. This improvement is attributed
538 to the complementary nature of wind and solar PV generation, as solar PV
539 typically peaks in summer while wind generation is more consistent in win-
540 ter. However, this integration is unable to counter the critical winter RES
541 droughts, which coincide with the strongest electricity demand in Northern
542 European countries like Ireland. Still, a more diversified renewable energy
543 mix mitigates extreme RES drought conditions and enhances overall system
544 resilience.

545 The results presented in this study have four main limitations. First, the
546 presented study uses a fixed threshold to define RES drought events, but
547 other methods could yield different results, even though the main takeaways
548 would be expected to be the same. Second, the definition of RES droughts
549 based on generation does not consider the mismatch between renewable gen-
550 eration and demand, which may be of interest to system operators, as these

551 events put large amounts of strain on the system. Third, the availability of
552 solar PV data is limited to a relatively short time period, as recent expan-
553 sions in installed capacity have significantly changed the generation land-
554 scape. Lastly, the source for weather data is ERA5, which is among the best
555 reanalysis datasets for renewable energy applications, but still comes in a
556 limited spatial resolution.

557 Future work is planned to extend the current analysis. First, climate pro-
558 jection data will be integrated with different energy scenarios, incorporating
559 the addition of offshore wind, to better understand how climate change might
560 affect RES droughts. Second, expanding the geographic domain of the study
561 to include the rest of Europe would provide a more comprehensive under-
562 standing of RES droughts in an interconnected electricity grid. This would
563 require extensive verification across other European countries, making it a
564 more complex but highly relevant challenge.

565 Data Availability

566 The ERA5 data can be obtained from the Climate Data Store (<https://doi.org/10.24381/cds.adbb2d47>). The C3S datasets are also available
567 from the Climate Data Store (<https://doi.org/10.24381/cds.4bd77450>).
568 Information on wind and solar PV farms in Ireland can be obtained from
569 the EirGrid website (<https://www.eirgrid.ie/grid/system-and-renewable-data-reports>). The Atlite model used in this study is open-source
570 and can be found on GitHub (<https://github.com/pypsa/atlite>). The
571 data and code required to reproduce the analysis in this article will be made
572 available upon acceptance of the manuscript in a public GitHub repository.
573
574

575 Acknowledgments

576 The research conducted in this publication was funded by Science Foun-
577 dation Ireland and co-funding partners under grant number 21/SPP/3756
578 through the NexSys Strategic Partnership Programme.

579 References

- 580 [1] EuroStat, Renewable Energy Statistics, 2023. URL: https://ec.europa.eu/eurostat/statistics-explained/index.php?title=Renewable_energy_statistics, Accessed: 2024-11-06.
581
582

- 583 [2] H. C. Bloomfield, D. J. Brayshaw, L. C. Shaffrey, P. J. Coker, H. E.
584 Thornton, Quantifying the increasing sensitivity of power systems to
585 climate variability, *Environmental Research Letters* 11 (2016) 124025.
586 doi:10.1088/1748-9326/11/12/124025.
- 587 [3] H. C. Bloomfield, D. J. Brayshaw, A. Troccoli, C. M. Goodess, M. De Fe-
588 lice, L. Dubus, P. E. Bett, Y.-M. Saint-Drenan, Quantifying the
589 sensitivity of european power systems to energy scenarios and cli-
590 mate change projections, *Renewable Energy* 164 (2021) 1062–1075.
591 doi:10.1016/j.renene.2020.09.125.
- 592 [4] F. Kaspar, M. Borsche, U. Pfeifroth, J. Trentmann, J. Drücke, P. Becker,
593 A climatological assessment of balancing effects and shortfall risks of
594 photovoltaics and wind energy in germany and europe, *Advances in
595 Science and Research* 16 (2019) 119–128. doi:10.5194/asr-16-119-2
596 019.
- 597 [5] F. Mockert, C. M. Grams, T. Brown, F. Neumann, Meteorological
598 conditions during periods of low wind speed and insolation in Germany:
599 The role of weather regimes, *Meteorological Applications* 30 (2023)
600 e2141. doi:10.1002/met.2141.
- 601 [6] M. Ohba, Y. Kanno, D. Nohara, Climatology of dark doldrums in japan,
602 *Renewable and Sustainable Energy Reviews* 155 (2022) 111927. doi:10
603 .1016/j.rser.2021.111927.
- 604 [7] M. J. Mayer, B. Biró, B. Szücs, A. Aszódi, Probabilistic modeling of
605 future electricity systems with high renewable energy penetration using
606 machine learning, *Applied Energy* 336 (2023) 120801. doi:10.1016/j.
607 apenergy.2023.120801.
- 608 [8] D. Raynaud, B. Hingray, B. François, J. Creutin, Energy droughts from
609 variable renewable energy sources in European climates, *Renewable
610 Energy* 125 (2018) 578–589. doi:https://doi.org/10.1016/j.renene
611 .2018.02.130.
- 612 [9] A. Gangopadhyay, A. K. Seshadri, N. J. Sparks, R. Toumi, The role
613 of wind-solar hybrid plants in mitigating renewable energy-droughts,
614 *Renewable Energy* 194 (2022) 926–937. doi:10.1016/j.renene.2022.
615 05.122.

- [10] J. Kapica, J. Jurasz, F. A. Canales, H. Bloomfield, M. Guezgouz, M. De Felice, Z. Kobus, The potential impact of climate change on european renewable energy droughts, *Renewable and Sustainable Energy Reviews* 189 (2024) 114011. doi:10.1016/j.rser.2023.114011.
- [11] K. Z. Rinaldi, J. A. Dowling, T. H. Ruggles, K. Caldeira, N. S. Lewis, Wind and Solar Resource Droughts in California Highlight the Benefits of Long-Term Storage and Integration with the Western Interconnect, *Environmental Science and Technology* 55 (2021) 6214–6226. doi:10.1021/acs.est.0c07848.
- [12] P. T. Brown, D. J. Farnham, K. Caldeira, Meteorology and climatology of historical weekly wind and solar power resource droughts over western North America in ERA5, *SN Applied Sciences* 3 (2021) 814. doi:10.1007/s42452-021-04794-z.
- [13] S. Allen, N. Otero, Standardised indices to monitor energy droughts, *Renewable Energy* 217 (2023) 119206. doi:10.1016/j.renene.2023.119206.
- [14] C. Bracken, N. Voisin, C. D. Burleyson, A. M. Campbell, Z. J. Hou, D. Broman, Standardized benchmark of historical compound wind and solar energy droughts across the Continental United States, *Renewable Energy* 220 (2024) 119550. doi:https://doi.org/10.1016/j.renene.2023.119550.
- [15] H. Lei, P. Liu, Q. Cheng, H. Xu, W. Liu, Y. Zheng, X. Chen, Y. Zhou, Frequency, duration, severity of energy drought and its propagation in hydro-wind-photovoltaic complementary systems, *Renewable Energy* (2024) 120845. doi:10.1016/j.renene.2024.120845, 2.
- [16] H. Hersbach, B. Bell, P. Berrisford, S. Hirahara, A. Horányi, J. Muñoz-Sabater, J. Nicolas, C. Peubey, R. Radu, D. Schepers, et al., The ERA5 global reanalysis, *Quarterly Journal of the Royal Meteorological Society* 146 (2020) 1999–2049. doi:10.1002/qj.3803.
- [17] L. Dubus, Y. Saint-Drenan, A. Troccoli, M. De Felice, Y. Moreau, L. Ho-Tran, C. Goodess, R. Amaro E Silva, L. Sanger, C3S Energy: A climate service for the provision of power supply and demand indicators for Europe based on the ERA5 reanalysis and ENTSO-E data, *Meteorological Applications* 30 (2023) e2145. doi:10.1002/met.2145.

- 650 [18] F. Hofmann, J. Hampp, F. Neumann, T. Brown, J. Hörsch, Atlite: a
651 lightweight Python package for calculating renewable power potentials
652 and time series, *Journal of Open Source Software* 6 (2021) 3294. doi:10
653 .21105/joss.03294.
- 654 [19] A. Kies, B. U. Schyska, M. Bilousova, O. El Sayed, J. Jurasz,
655 H. Stoecker, Critical review of renewable generation datasets and their
656 implications for european power system models, *Renewable and Sus-
657 tainable Energy Reviews* 152 (2021) 111614. doi:10.1016/j.rser.202
658 1.111614.
- 659 [20] EirGrid & SONI, System and Renewable Data Reports, 2023. URL:
660 [https://www.eirgrid.ie/grid/system-and-renewable-data-rep](https://www.eirgrid.ie/grid/system-and-renewable-data-reports)
661 [orts](https://www.eirgrid.ie/grid/system-and-renewable-data-reports), Accessed: 2024-11-06.
- 662 [21] Y.-M. Saint-Drenan, L. Wald, T. Ranchin, L. Dubus, A. Troccoli, An
663 approach for the estimation of the aggregated photovoltaic power gener-
664 ated in several European countries from meteorological data, *Advances
665 in Science and Research* 15 (2018) 51–62. doi:10.5194/asr-15-51-201
666 8.
- 667 [22] I. Staffell, S. Pfenninger, Using bias-corrected reanalysis to simulate
668 current and future wind power output, *Energy* 114 (2016) 1224–1239.
669 doi:10.1016/j.energy.2016.08.068.
- 670 [23] Government of Ireland, Climate Action Plan 2024, Technical Report 3,
671 Department of the Environment, Climate and Communications, 2023.
672 URL: [https://www.gov.ie/pdf/?file=https://assets.gov.ie/](https://www.gov.ie/pdf/?file=https://assets.gov.ie/284675/70922dc5-1480-4c2e-830e-295afd0b5356.pdf)
673 [284675/70922dc5-1480-4c2e-830e-295afd0b5356.pdf](https://www.gov.ie/pdf/?file=https://assets.gov.ie/284675/70922dc5-1480-4c2e-830e-295afd0b5356.pdf), Accessed:
674 2024-11-06.
- 675 [24] Sustainable Energy Authority Ireland, National Energy Projections
676 2024, Technical Report, Sustainability Energy Authority of Ireland,
677 2024. URL: [https://www.seai.ie/news-and-events/news/energ](https://www.seai.ie/news-and-events/news/energy-projections-report)
678 [y-projections-report](https://www.seai.ie/news-and-events/news/energy-projections-report), Accessed: 2024-11-06.
- 679 [25] H. G. Beyer, G. Heilscher, S. Bofinger, A robust model for the mpp
680 performance of different types of pv-modules applied for the performance
681 check of grid connected systems, *Eurosun* (2004) 8.